



Characterization of the carbon erosion on the limiter of Tore Supra

E. Delchambre^{a,*}, A. Beaute^a, S. Brezinsek^b, S. Carpentier^a, Y. Corre^a, G. Dunand^a, A. Ekedahl^a, A. Escarguel^c, J. Gunn^a, Y. Marandet^c, V. Moncada^a, P. Monier-Garbet^a, J.M. Traverre^a, E. Tsitrona^a, B. Pegourie^a

^a Association EURATOM CEA, CEA Cadarache, CEA-DSM-DRFC, F-13108 St. Paul lez Durance, France

^b Institut für Energieforschung, Plasmaphysik, Trilateraler Euregio Cluster, EURATOM Association, 52425 Jülich, Germany

^c Laboratoire PIIIM, Université de Provence, Ave Escadrille Normandie Niemen, Marseille, France

ARTICLE INFO

PACS:
33.20.Kf
28.52.–s
29.30.–h

ABSTRACT

This paper focuses on chemical erosion characterisation at Tore Supra by visible spectral analysis of carbon and deuterium transitions at the toroidal pumped limiter – the main source of carbon. A new image-processing tool for visible imaging analysis allows to identify carbon sources on the limiter. Spectrally resolved data have been also obtained on the limiter in particular the observation of the CD band (Gerö band), related to chemical erosion. Erosion yields have been assessed and chemical erosion represents roughly 30% of the total carbon erosion.

© 2009 Elsevier B.V. All rights reserved.

1. Introduction

Erosion of carbon plasma-facing components in ITER has a strong impact on their lifetime as well as on tritium retention through codeposition processes [1]. The database for chemical erosion at high fluxes and fluences and at low surface temperatures is still uncertain, therefore dedicated experiments in Tore Supra were carried to study the chemical erosion of actively cooled plasma-facing components (PFC) at electron temperatures at $T_e = 20\text{--}40$ eV, where chemical erosion is expected to be high according to Roth Formula [2]. In addition to infrared endoscopes, a visible camera equipped with multiple interference filters (D_α , $\text{CII}_{515\text{nm}}$ and CD (Gerö band)) views the toroidal pump limiter (TPL). This set-up allows comparing the spatial distribution of recycling and impurity fluxes emitted from deposition/erosion areas to the heat load pattern measured with an IR camera. The diagnostic system is completed by spectrally resolved measurements, in order to assess the chemical and physical sputtering yields.

2. Experimental set-up

The direct imaging system consists of a single CCD camera using a filter wheel, and allows to monitor from the top part of the machine 15° of the toroidal section of the TPL which roughly corresponds to one period of the heat pattern on the limiter. The system is coupled with a vertical array of four optical fibres linked to a Czerny–Turner spectrometer. The optical fibre set allows to

cross compare the spectrally filtered camera data with spectrally resolved spectrometer data from the same observation area. The particle influx is obtained from the absolutely calibrated brightness using the standard procedure for ionising plasmas [3], that is the number of ionization per photon of the relevant transition (factor S/XB where S stands for the ionization rate coefficient of an atom and XB is the excitation rate coefficient of the observed transition weighted with the branching ratio). The S/XB values are obtained using ADAS [4] for a given set of electron density n_e and temperature T_e . n_e and T_e in the ionization volume are deduced from Reciprocating Langmuir Probe (RP) measurements in the top part of the machine (via the 3D magnetic configuration). The TPL is also monitored by infrared cameras. This combination of edge diagnostics allows detailed spatial study of the carbon erosion on the TPL. A quantitative image analysis software has been recently developed, WOLFF (Warping toOL For Fusion), in order to study particle and heat fluxes on the TPL. Based on warping technique, the software enables to superimpose filtered images onto the real geometry of the observed object, as well as images taken with different angles of view [5].

3. Results

The combination of 3D magnetic configuration including ripple and heat flux folding length in the scrape of layer (SOL) defines the heat flux pattern [6] which is closely related to the erosion/deposition pattern. Two main erosion zones, electron (1) and ion (2) drift sides, are observed on the TPL as shown in Fig. 1(b). Deposition zones are localised on shadowed areas and also on the contact point (tangential area) between the limiter and the Last Closed

* Corresponding author.

E-mail address: elise.delchambre@cea.fr (E. Delchambre).

Flux surface (LCFS) according to observations made with the visible camera. It was previously observed that bright areas in the visible (H_α emission, signature of the plasma limiter interaction) correspond to the heat flux foot prints [7]. The superimposition of H_α images from erosion experiments (Fig. 1(a)) over the TPL geometry (Fig. 1(b)) have shown an unexpected emission pattern compared to the erosion areas. Indeed H_α emission is observed mostly on the erosion zone (1) and surprisingly on the tangential zone too (contact point between the LCFS and the limiter). There is no emission maximum in erosion zone (2). Moreover CD (related to chemical erosion) and CII are observed on both erosion zones as shown in Fig. 2 and also on the tangential zone.

On the contrary when the LCFS is 2 cm away from the limiter, a 'standard' emission (on erosion zones 1 and 2 only) is observed for CD and CII. The emission observed on the tangential zone appears when the LCFS is connected to the TPL (which is the standard plasma configuration) and highlights a strong recycling and plasma wall interaction going on in this region. This observation is in agreement with IR analysis observing strongly heated deposits in this region [8] which are more or less attached to the bulk and tend to overheat. The presence of deposits at the zone of tangency is consistent with TEXTOR results on the Alt-II limiter [9], and the change of emission pattern might be related to successive growth and flaking of these deposits.

Repetitive discharges have been performed (ohmic discharge, $I_p = 1$ MA, $n_i \sim 4 \times 10^{19} \text{ m}^{-3}$, $n_e = 0.8 \times 10^{19} \text{ m}^{-3}$ at the LCFS, $T_{\text{surf}} = 400\text{--}500$ K on erosion zone) in order to analyse chemical erosion with a scan in radiated fraction. This attempt unexpectedly led to detachment, and highlights the occurrence of a radiative instability called MARFE (Multi-faceted Asymmetric Radiation From the Edge) with a precursor of CII emission on the tangential zone as shown in Fig. 3 (no increase of H_α is observed). Indeed, an increase of CII and CD on thick deposits area is measured before detachment, while during detachment emission drops on erosion zones both for CD, CII and $D\alpha$. This tends to suggest that detachment is triggered by deposit erosion or outgassing which can locally increase the density and may provide a hint about the role of deposits in disruptions. It is worth noting that this does not occur when the LCFS is 2 cm away from the TPL.

During this experiment the CD band was spectrally resolved on the optical fiber views (see Fig. 1(b)), as shown in Fig. 4, and evidenced the presence of chemical erosion, at least partially validating imaging data in CD light. The chemical erosion yield, Y_{chem} , can

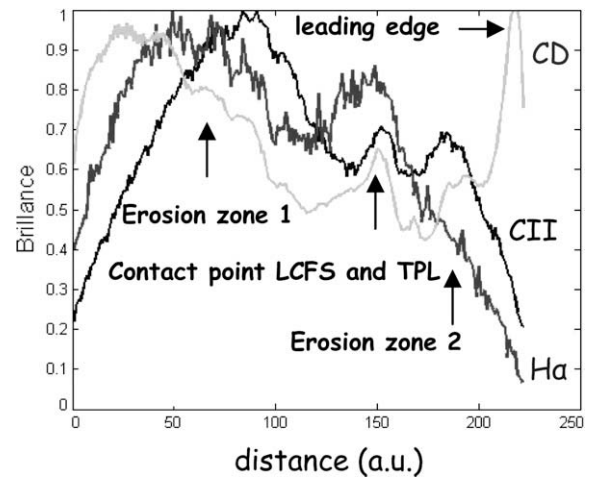


Fig. 2. CII, H_α and CD profiles on the limiter along the line shown in Fig. 1.

be calculated from $CD/D\gamma$ fluxes and can be compared to the total erosion yield, Y_{tot} , deduced from $CII/D\gamma$. Since the sensitivity of the detector in CD region (431 nm) is rather low (10 times lower than H_α region), an integration time of 3 s is required. Erosion calculation has been first made during quiescent plasma, when the LCFS is 2 cm away from the TPL (shots #38805 and #38806). On the erosion zone (corresponding to fibre 3), $T_e \sim 20$ eV, $n_e \sim 0.8 \times 10^{19} \text{ m}^{-3}$ and the deuterium flux is $3 \times 10^{21} \text{ D/m}^2/\text{s}$, from projection of RP data on the TPL, therefore ionization per photon can be calculated for each species: $[D/XB]_{CD4-CD} = 56$ for the complete CD A–X band [10], $[S/XB]_{CII(426\text{nm})} = 20$, $[S/XB]_{H\gamma} = 1300$ including a correction for the molecular contribution [11]. The emission ratio $CII_{(426\text{nm})}/D\gamma$ and $CD/D\gamma$ are measured on the same spectra in order to avoid calibration uncertainties. Particle fluxes are calculated for each species from the line brightness, L , with $\Phi = 4 \cdot \pi \cdot L \cdot S/XB$. The deuterium flux calculated from $D\gamma$ gives $\Phi_D = 1.8\text{--}3.8 \times 10^{21} \text{ D/m}^2/\text{s}$ which is in good agreement with RP data. The total erosion rate $CII_{(426\text{nm})}/D\gamma$ in this region is found to be of about $\sim 4\%$ and $CD/D\gamma \sim 1.3\%$. We can deduce that $Y_{\text{chem}}/Y_{\text{tot}}$ is roughly $\sim 25\text{--}30\%$. When the LCFS is connected to the TPL (shots #38799 and #38803), we still obtain $Y_{\text{chem}}/Y_{\text{tot}} \sim 30\%$ with $CII_{(426\text{nm})}/D\gamma \sim 5\%$ and $CD/D\gamma \sim 1.5\%$. Due to the strong dependence of S/XB with plasma parameters (n_e, T_e) which varies along the discharge and the

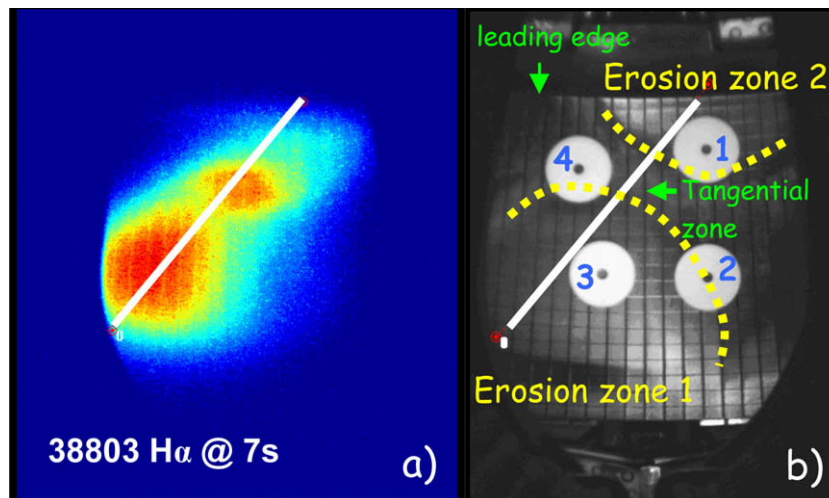


Fig. 1. Image of the limiter taken with (a) H_α filter (b) no plasma no filter. The four circles materialises optical fibres views. Line profile is represented in white in both figures, dashed lines mark the boundary of erosion zones.

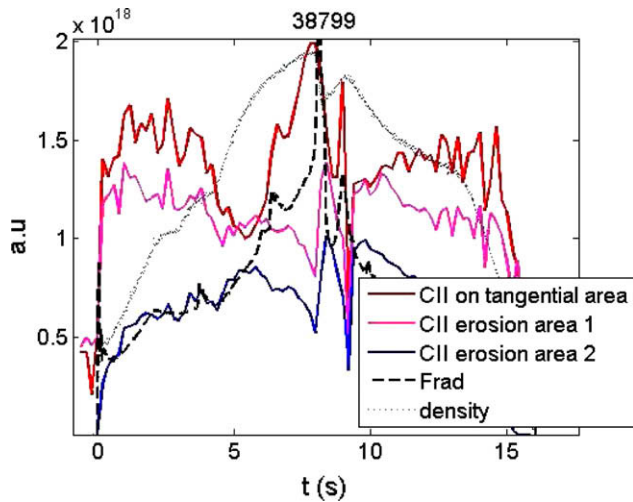


Fig. 3. Time evolution of CII on erosion zone (1&2) and contact between the LCFS and the TPL (3) compared with radiated fraction (F_{rad}) and plasma density.

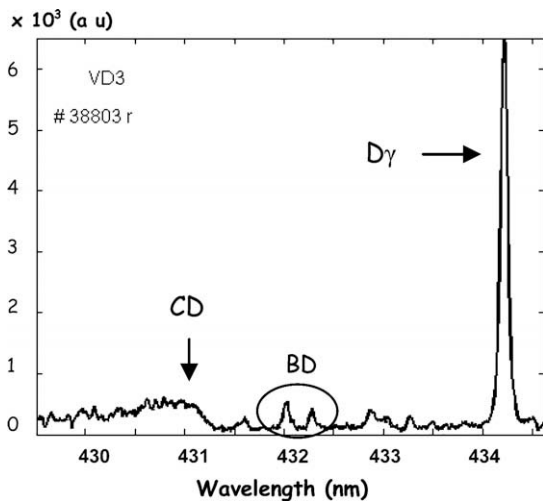


Fig. 4. Spectrum of CD band measured during the plasma discharge, with 3 s of integration time (before the MARFE) on the region covered by the fibre 3 (see Fig. 1b).

lines of sight, and considering the long integration times (3 s) for CD band acquisition, those values should be taken with caution. Indeed plasma parameters profiles should be taken into consider-

ation whereas S/XB values for the local parameters at the maximum of emission were used.

4. Discussion and conclusion

The new image-processing tool WOLFF represents a significant improvement for visible imaging spectroscopy, in particular to compare heat load pattern and atomic/molecular emission and to identify carbon sources on the limiter. It highlighted that limiter plasma interaction have changed since 2003 [6] probably due to the surface state modification (deposits in the area where magnetic field lines are tangential to the TPL). Correlation with CII emission on deposits region and occurrence of detachment has been observed. Since MARFE increases the density (close to the density limit) which can generate disruption, this observation is of great interest to better understand the link between deposits and disruption via the release of impurity trapped in carbon deposits. Chemical erosion has been observed and seems to represent roughly 30% of the total erosion. However, the reliability of the measure could be improved by improving calibration procedure and performing discharges with steady state plasma conditions (n_e, T_e). Total carbon flux from spectroscopic data can be calculated but can lead to a significant overestimate of carbon eroded. Indeed spectroscopy only measures gross erosion since part of the carbon observed is locally redeposited and does not contribute to the large carbon net erosion. The question of migration needs now to be investigated so as to assess net erosion/deposition rates, which are directly connected to components life time and codeposition, hence tritium retention.

Acknowledgements

The author acknowledges R. Mitteau and R. Guirlet for technical help and fruitful discussions.

References

- [1] E. Tsitrone et al., J. Nucl. Mater. 363 (2007) 12.
- [2] J. Roth, J. Nucl. Mater. 266 (1999) 51.
- [3] A. Pospieszczyk, Atomic and Plasma–Material Interaction Processes in Controlled Thermonuclear Fusion, Elsevier Science Publishers, 1993.
- [4] <<http://www.adas.ac.uk>>.
- [5] E. Delchambre et al., in: AIEA Workshop on Plasma Spectroscopy, Jaipur, 2007.
- [6] R. Mitteau et al., J. Nucl. Mater. 266 (1999) 798.
- [7] R. Mitteau et al., J. Nucl. Mater. 313 (2003) 1229.
- [8] S. Carpentier, these Proceedings.
- [9] P. Wienhold et al., J. Nucl. Mater. 313 (2003) 311.
- [10] S. Bresinsek et al., J. Nucl. Mater. 363 (2007) 1119.
- [11] A. Azéroual et al., Nucl. Fus. 40 (2000) 1651.